Cardiovasc Intervent Radiol (2023) 46:128–135
https://doi.org/10.1007/s00270-022-03301-0

LABORATORY INVESTIGATION NON-VASCULAR INTERVENTIONS

Robot-Assisted Needle Insertion for CT-Guided Puncture: Experimental Study with a Phantom and Animals

Xiangqian Chen[1] · Yadong Yan[2] · Ailing Li[3] · Tianmiao Wang[1] · Yu Wang[2]

Received: 16 June 2022 / Accepted: 11 October 2022 / Published online: 15 November 2022

Abstract
Purpose This study aimed to evaluate the accuracy and safety of robotic CT-guided needle insertion in phantom and animal experiments.
Materials and Methods A robotic system was developed for CT-guided needle insertion. For the phantom experiment, a specially made phantom containing multiple spherical was used. 15 robotic and manual insertions were conducted, and the accuracy, time, number of needle insertions, and radiation dose were compared between the robotic and manual insertion using Student's *t*-test. For the animal experiment, 20 robotic needle insertions were attempted toward simulated pulmonary nodules in the swine lung. The accuracy and safety of robotic CT-guided needle insertions were evaluated.
Results In the phantom experiment, the mean accuracies of manual and robotic insertion were 1.8 ± 0.3 mm and 1.9 ± 0.2 mm. The accuracy of robotic needle insertion had no significant difference with manual needle insertion, but the number of needle insertions and radiation dose of the robotic needle placement significantly decreased compared to manual needle placement. In the animal experiment, the mean accuracy of the robotic needle insertion was 3.8 ± 1.3 mm. The time for the whole needle insertion was 14.4 ± 4.8 min. The whole robotic needle insertions were safe and only one mild pneumothorax occurred.
Conclusion CT-guided robotic needle insertion showed accuracy comparable to manual needle insertion, but the number of needle insertions, confirmatory scans, and radiation exposure had been reduced significantly. In future, we will further apply the robotic system to clinical experiments.

Keywords CT-guided puncture · Robotic CT-guided needle insertion · Phantom experiment · Animal experiment

Introduction

With the rapid development of imaging interventional technology, percutaneous CT-guided puncture has become one of the most commonly used interventional methods [1–3]. Such procedures include biopsy [4], ablation [5], drainage [6], and preoperative marking [7]. However, traditional percutaneous CT-guided puncture relies on the physician's experience and requires multiple CT scans and punctures, resulting in a significant radiation burden to the patient [8, 9].

In recent years, the development of navigation robot technology has provided a new solution for percutaneous interventions [10]. By combining CT and 3D reconstructed images, the robot system can reduce the difficulty of needle placement and improve the accuracy [11–13]. Especially

✉ Yu Wang
wangyu@buaa.edu.cn

1 School of Mechanical Engineering and Automation, Beihang University, Beijing, China

2 School of Biological Science and Medical Engineering, Beihang University, No. 37 Xueyuan Road, Haidian District, Beijing 100191, People's Republic of China

3 Beijing TrueHealth Medical Technology Co., Ltd., Beijing, China

for highly inaccessible targets that require multiple plane angulations, by using off-axial paths of needle placement, the robot system can improve access to the target [14]. Smakic et al. [15] evaluated commercial robot-assisted puncture equipment (MAXIO, Perfint healthcare, India) for CT-guided diagnostic and therapeutic interventions. They found that high precision can be achieved by using robot-assisted devices in out-of-plane CT-guided interventions compared with manual placement. Groetz et al. [16] reported their experience of performing CT-guided biopsy of bone by using a robot-assisted device (iSYS Medizintechnik GmbH, Kitzbuehel, Austria). They concluded that using the iSYS robot can improve the precision and convenience of biopsy of orthopedic lesions and avoid multiple needle adjustment. Hiraki et al. [17, 18] developed a remote-controlled 6-dof robotic system called "Zerobot", which can locate and insert a needle accurately under CT guidance. They conducted phantom experiments and animal experiments to evaluate the accuracy of the robotic system. All these studies show that interventional robotic systems have attracted great attention in interventional radiology and have also achieved some satisfactory results in experimental verification.

In this study, we developed a robotic system that can perform 3D navigation and assist in accurate needle placement. To evaluate the stability and accuracy of the system, an experiment of robotic assisting needle placements was performed in a phantom comparison to manual placement by experienced interventional radiology physicians. Animal experiments were also conducted to evaluate the safety of the system.

Materials and Methods

Robotic System

The interventional robotic system, a prototype system of Beijing TrueHealth Medical Technology Co., Ltd. produced for preclinical studies on a phantom and animals, is an image-guided navigation device that can help the physician to perform puncture under the guidance of CT (Fig. 1). The prototype system consists of hardware modules and software modules. The main hardware modules include the robot arm, photoelectric navigation device, workstation, screen, trolley, needle guide, etc. The main software modules include image processing, registration, respiratory monitoring, planning and control.

Specifically, the hardware of the prototype system consists of the following four modules: a robotic arm trolley positioned next to the patient, with a six degrees of freedom (6-dof) robotic arm (UR5, Universal Robots, Denmark); a console trolley positioned opposite to the robotic arm trolley, with a workstation, two screens and a photoelectric navigation device (NDI Polaris Vega, Ontario, Canada); a needle guide attached to the end of the robotic arm, which can fix the planned puncture path to define the needle insertion angle, needle insertion point and

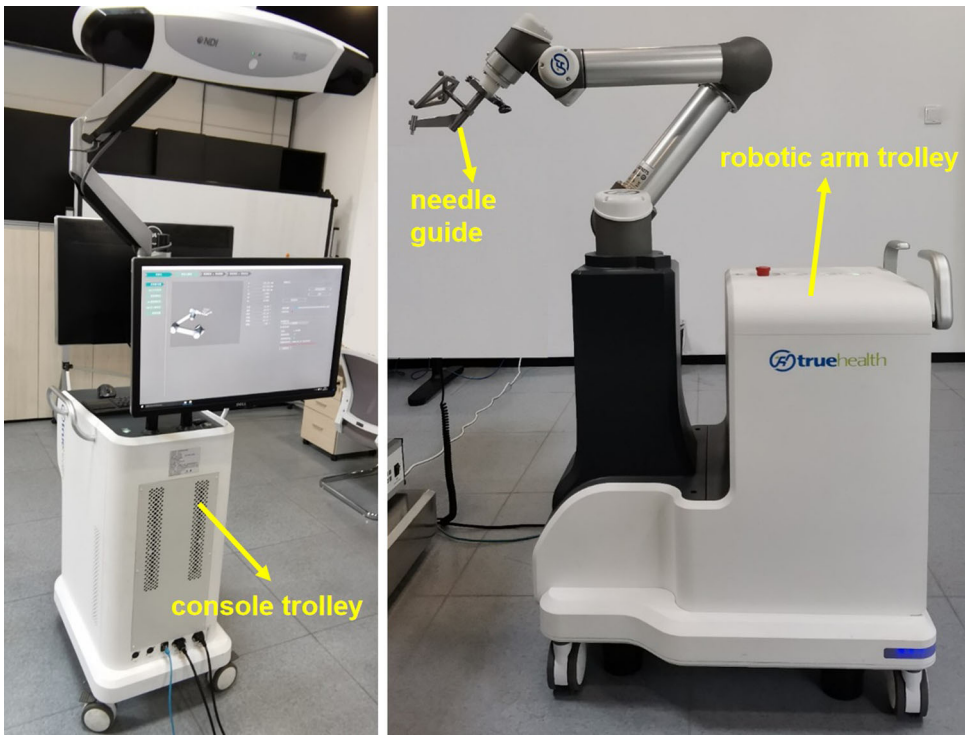

Fig. 1 Components of robotic system

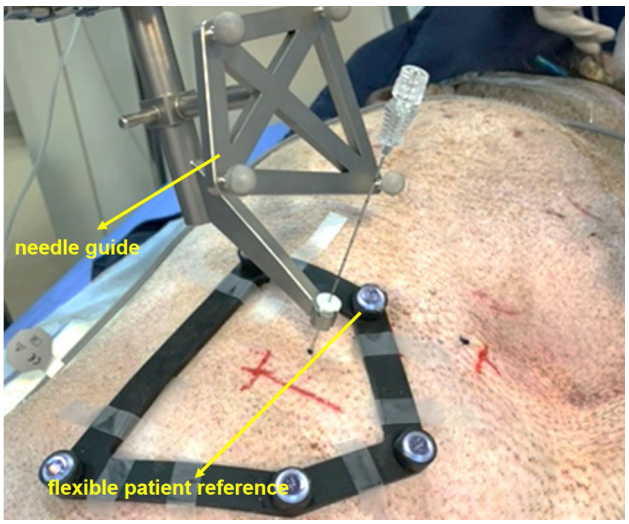

Fig. 2 Robotically assisted needle insertion

depth; and a flexible patient reference (Fig. 2) attached to the patient's skin to monitor the patient's breathing movements.

The software running on the prototype system also consists of four modules:

1. *Image processing module* This module can read and display DICOM data of the CT scan. The module supports the function of 3D reconstruction.
2. *Registration module* This module can automatically register the coordinate correspondence between the 3D reconstruction model and the real position of the patient by obtaining the CT image coordinates and real spatial coordinates of the flexible patient reference.
3. *Respiratory monitoring module* This module can track and display the respiratory cycle in real time, thus guiding the physician to complete the puncture at the optimal breathing phase. The extraction of the breathing curve is performed by real-time registration of the preoperative and intraoperative flexible patient reference (Fig. 3).
4. *Planning and control module* In this module, the physician can select the target and the skin entry point according to the CT and 3D reconstruction images, and the system automatically forms a puncture path.

Phantom Experiment

A phantom experiment was performed to compare manual needle insertion and robotic needle insertion. The phantom consisted of an acrylic box (200 × 150 × 150 mm) and a tracker fixed on the box used for registration. The acrylic box contained a layer of silicone on the surface and a layer of gelatin on the inside. The silicone on the surface of the phantom was used to simulate human skin, and the gelatin inside was used to simulate a human lung. The phantom contained 16 radiopaque spherical targets with a diameter of 8 mm, used to mimic lesions.

Experimental Procedure for Manual Needle Insertion

An IR physician with 10 years of experience in CT-guided needle insertion participated in the experiment. First, a baseline CT of the phantom was conducted. The physician chose one of the radiopaque spheres as the puncture target by viewing the CT scan (Fig. 4a). Then, the physician performed a puncture by using an 18-G*200-mm needle (Hakko SONOGUIDE PTC NEEDLE, Hakko Co., Ltd, Japan). When the puncture was complete, CT was repeated to observe the corresponding position of the puncture needle and target. If the position of the needle was ideal, the puncture was completed. The ideal needle position meant that the puncture needle reached the center of the spherical target, and the physician would determine whether the puncture position was ideal. Otherwise, the position of the puncture needle was readjusted until the position was satisfactory.

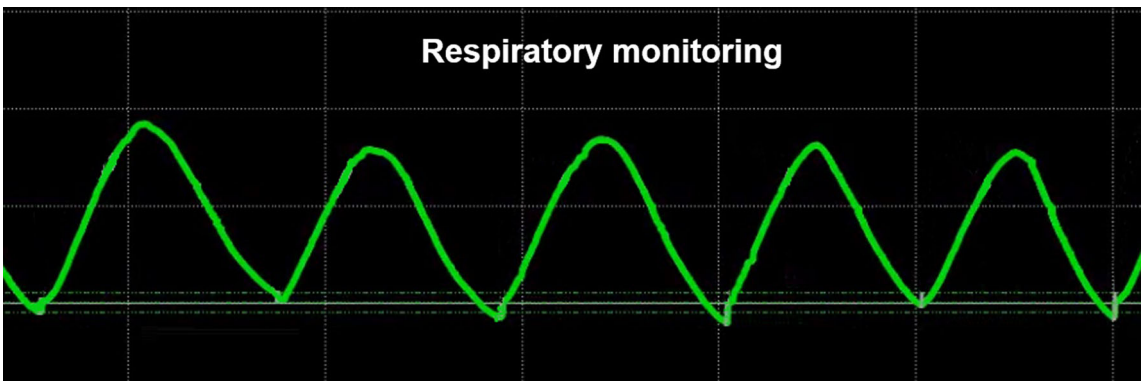

Fig. 3 The curve of respiratory monitoring

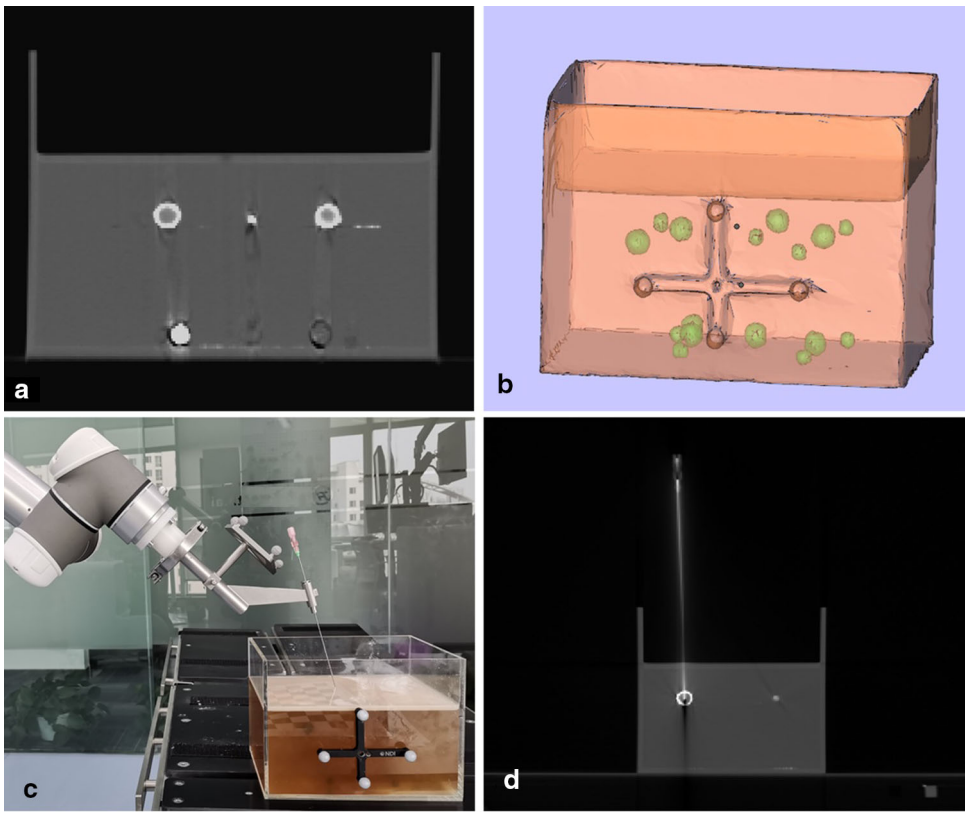

Fig. 4 The Phantom experiment. **a** The baseline CT of phantom. **b** The three-dimensional (3D) model of phantom. **c** Robotic-assisted puncture. **d** The final confirmatory CT

Experimental Procedure for Robot-Assisted Needle Insertion

The IR physician also participated in the robot experiment. The procedure started with baseline CT DICOM data acquisition, and the acquired CT was transferred to the image processing module to perform three-dimensional (3D) reconstruction (Fig. 4b). Next, puncture path planning was performed with the planning and control modules based on the position of the radiopaque spherical target in the 3D visualization model. The robotic arm performed the positioning operation and fixed the needle insertion angle, needle insertion point and depth. Finally, the physician performed the puncture with the aid of the robotic arm (Fig. 4c).

Data Collection and Analysis

In the phantom experiment, manual needle insertion and robotic insertion were performed 15 times each. For each insertion, the accuracy, total procedure time, number of needle insertions and radiation dose were collected. Radiation exposure was calculated by Dose Length Product (DLP), which was used to evaluate the total radiation dose of CT scan in a patient's treatment, and it was the patient who was exposed to radiation. The final confirmatory CT (Fig. 4d) scan was used to calculate the accuracy of needle insertion. The accuracy of needle insertion was calculated by measuring the distance between the needle tip and the target center. The needle insertion time was measured from the initial CT scan to the completion of puncture.

This study used a two-sided test level with $P < 0.05$ considered statistically significant. All statistical analyses were performed using SPSS statistical software (version 19.0; IBM SPSS, Armonk, New York).

Animal Experiment

Four adult male Guangxi Bama miniature pigs were used in this experiment. The Experimental Animal Ethics Committee of Silver Snake (Guangzhou) Medical Technology Co., Ltd. reviewed and approved the experimental protocol.

Experimental Procedure

In the experiment, octyl-α-cyanoacrylate (Baiyun medical glue, China) was used to generate simulated nodules. After simulated nodule formation, a CT scan was conducted to acquire the DICOM data. Then, 3D visualization models of the skin, lungs, ribs, fiducial markers, bronchi and blood vessels were all reconstructed. By using the photoelectric navigation device, the real spatial position information of the pig was registered with the corresponding 3D

Fig. 5 The process of robotic positioning and assisted puncture

visualization models in the software system. Next, the physician could plan a safe puncture path that was automatically performed by the robotic arm. Meanwhile, the respiratory monitoring module tracked the respiratory cycle of the pig in real time. When the breathing curve reached its lowest point, the breathing of the pig was stopped by the ventilator, and the physician inserted the needle through the skin and pushed it into a predetermined depth with the help of the needle guide (Fig. 5). Finally, when the needle was in place, the pig's breathing was restored, and confirmatory CT was performed to assess the targeting accuracy.

Data Collection

For this experiment, the positioning accuracy, positioning time and safety were collected. The accuracy of positioning accuracy was measured by calculating the distance between the edge of the simulated nodule and the needle tip. The positioning time was calculated from the start of the CT scan to the completion of puncture. Safety was evaluated by adverse events related to puncture, such as pneumothorax and hemothorax.

Results

Phantom Experiment

The results of the phantom experiment are shown in Table 1. The mean accuracies of manual and robotic needle insertion were 1.8 ± 0.3 mm and 1.9 ± 0.2 mm ($P = 0.43$). The mean needle insertion time was 5.0 ± 1.3 min for the manual group versus 5.8 ± 1.5 min for the robotic group ($P = 0.27$). However, statistically significant variations were observed in the number of needle insertions ($P < 0.001$) and radiation dose ($P < 0.05$). The number of needle insertions and radiation dose to the phantom for the manual group were 2.7 ± 1.0 and 567.1 ± 87.2 mGy*cm, respectively, while for the robotic group they were 1.1 ± 0.3 and 172.7 ± 17.9 mGy*cm.

Animal Experiment

A total of 4 pigs with 20 nodules were located in the experiment. The results of the animal experiment are shown in Table 2, and CT images from the animal experiment are shown in Fig. 6. The mean accuracy of the robotic needle insertions was 3.8 ± 1.3 mm. The positioning time was 14.4 ± 4.8 min.

One case of pneumothorax occurred in this experiment, for an incidence rate of 5.00% (1/20). The pneumothorax

Table 1 Results of the phantom experiment

	Manual insertion	Robotic insertion	*P* value
Needle insertion accuracy (mm)	1.8 ± 0.3	1.9 ± 0.2	0.41
Needle insertion time (min)	5.4 ± 1.3	5.8 ± 0.8	0.21
No. of needle insertions	2.7 ± 1.0	1.1 ± 0.3	< 0.001
Radiation dose to phantom (DLP, mGy*cm)	561.7 ± 87.2	172.7 ± 17.9	< 0.001

Table 2 Results of the animal experiment

	Nodule	The diameter of nodule (mm)	Positioning accuracy (mm)	Positioning time(min)
Pig No. 1				
Left lung	1	0.9	1.7	21
	2	0.6	4.4	23
	3	0.6	4.0	23
Right lung	1	0.8	1.9	20
	2	0.7	3.4	13
	3	0.7	2.8	16
Pig No. 2				
Left lung	1	0.6	5.9	16
Right lung	1	0.9	4.9	16
	2	0.6	3.9	13
Pig No. 3				
Left lung	1	0.8	3.8	13
	2	0.8	4.1	10
Right lung	1	0.5	6.2	12
	2	0.5	2.6	10
	3	0.9	4.4	12
	4	0.9	1.5	12
Pig No. 4				
Left lung	1	0.9	3.9	10
	2	0.9	3.4	10
Right lung	1	0.9	3.4	8
	2	0.9	5.2	9
	3	0.7	4.6	20
Mean		0.8	3.8	14.4
Standard deviation		0.1	1.3	4.8

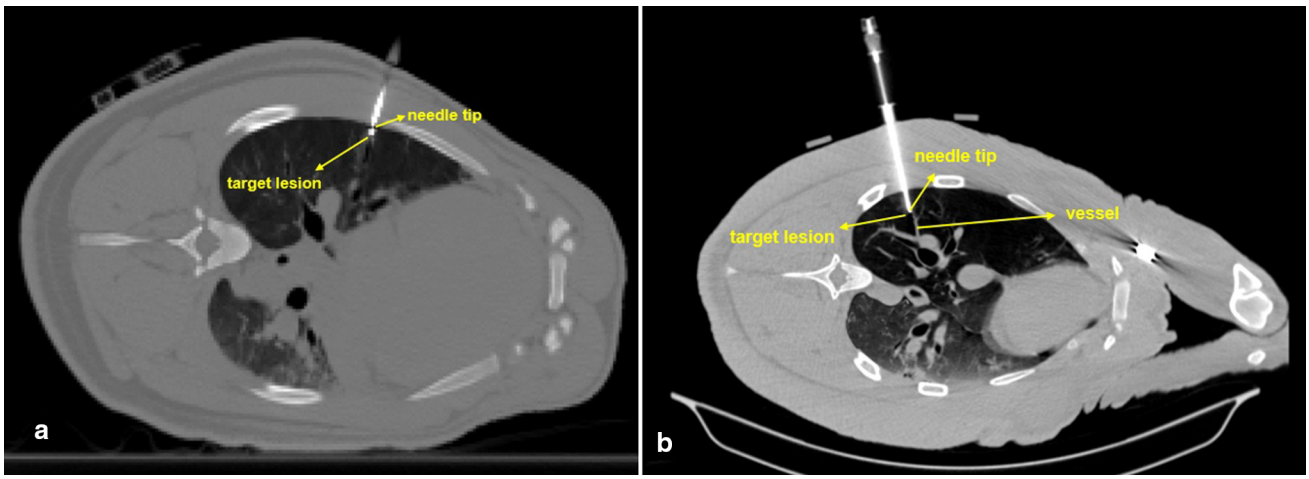

Fig. 6 CT images obtained after robotic needle insertion in the swine

was not severe. When the pneumothorax occurred, closed thoracic drainage was required for the pig, and continuous negative-pressure drainage was performed with a central venous catheter until no pneumothorax was confirmed. No

other adverse events, such as hemothorax, embolism, or death, occurred.

Discussion

There are currently several robotic systems for CT-guided interventions, such as Perfint [15], iSYS [16], Zerobot [17, 18] and EPIONE [19]. These existing robotic systems are mostly based on the coordinates of the CT image, which are directly mapped to the robotic arm to perform positioning, and the patient needs to strictly maintain a fixed position without moving. However, the patient is under local anesthesia in many puncture scenarios, and it is difficult to ensure that the patient not move during the entire puncture process. Compared with the above robotic systems, our prototype system may have the advantage of real-time tracking. By using a photoelectric navigation device to track the patient's position and the robotic arm in real time, the positioning accuracy may not be affected even if the patient moves during the puncture process. In addition, using a similar fiducial and a clip or fixed arm to assist CT-guided interventions is commonly used in the clinic [20, 21]. Compared with this method, this prototype system may be more convenient and accurate by using a robotic arm to perform positioning automatically. Another positioning method is electromagnetic navigation, such as the IG4 system (Veran Medical Technologies, America) [22]. Rather than electromagnetic navigation, the photoelectric navigation used in our robotic system has higher accuracy and stability. Another possible advantage of this prototype system could be the development of the respiratory monitoring module. For mostly existing robotic systems, the physician judges the breathing of the patient from experience and instructs the patient to hold the breath at a certain moment to make the puncture. Our respiratory monitoring module can track the patient's breathing in real time by a flexible patient reference and quantify the patient's breathing status. By automatically calculating the most matching puncture timing, it can accurately instruct the doctor to complete the puncture at the optimal time and overcome the influence of breathing on the puncture accuracy. In short, our robotic system has the advantage of integrating the three functions of robotic arm positioning, photoelectric navigation tracking and respiratory monitoring. It may have better adaptability and higher use value.

As for the occurrence of puncture complications, the incidence of pneumothorax was 5%. Pneumothorax may be caused by a tear in the lung caused by the puncture. Hiraki et al. [18] carried out puncture experiments on 5 pigs, and 1 case of minor pneumothorax appeared, which is also consistent with our results. Pneumothorax is a common complication of thoracic puncture. The complication rate for conventional manual needle insertion is approximately 15–25% [23, 24]. The complications are mainly caused by the puncture procedure itself, rather than by the robotic positioning technology. In fact, it can be seen from phantom experiments that the use of robotic positioning can significantly reduce the number of needle insertions (1.1 for the robotic group vs. 2.7 for the manual group), and fewer punctures should mean a lower incidence of complications [23]. Meanwhile, robot assistance can improve the accuracy of puncture, and avoid the puncture error caused by the doctor's hand shaking. So it will be very useful, likely in cases where lesion is near vessel or near diaphragm, showed in Fig. 6.

Our study has the following limitations. For the phantom experiment, although our phantom simulated the characteristics of skin and soft tissue, it could not simulate the state of human breath because the phantom was a static model. For the animal experiment, the pigs were under general anesthesia (because pigs cannot undergo local anesthesia), and we used a ventilator to control the pig's breathing by cutting off the airway based on a respiratory monitoring module. However, in many clinical interventional procedures, the patients are in the state of local anesthesia with autonomous breathing, and we need the patient to stop breathing according to the guide of the respiratory monitoring module, so the application effect of the respiratory monitoring module needs further clinical verification.

Conclusion

Our experiment showed that CT-guided robotic needle insertion showed accuracy comparable to that of manual needle insertion, but the number of needle insertions, confirmatory scans and radiation exposure for CT-guided robotic needle insertion were significantly lower. Animal experiments verified that robotic needle insertion was simple and safe, so the robotic system is a very effective tool to assist physicians in achieving accurate puncture, eliminating the dependence on puncture experience. In future, we will further apply the robotic system to clinical experiments.

Author Contributions XC designed the study and edited the final manuscript. YY and AL collected the data, performed a literature review, and produced the draft manuscript. TW helped with the writing of the manuscript. YW conceived the study. All authors have read and agreed to the published version of the manuscript.

Funding This study was funded by Beijing TrueHealth Medical Technology Co., Ltd.

Declarations

Conflict of interest The authors declare no conflict of interest.

Ethical Approval The animal experiment was approved by the Experimental Animal Ethics Committee of Silver Snake (Guangzhou) Medical Technology Co., Ltd.

Informed Consent For this type of study, informed consent is not required.

Consent for Publication For this type of study, consent for publication is not required.

References

1. Markelj P, Tomaževič D, Likar B, et al. A review of 3D/2D registration methods for image-guided interventions. Med Image Anal. 2012;16(3):642–61.
2. Phillips WT, Bao A, Brenner AJ, et al. Image-guided interventional therapy for cancer with radiotherapeutic nanoparticles. Adv Drug Deliv Rev. 2014;76:39–59.
3. Sarti M, Brehmer WP, Gay SB. Low-dose techniques in CT-guided interventions. Radiographics. 2012;32(4):1109–19.
4. Tai R, Dunne RM, Trotman-Dickenson B, et al. Frequency and severity of pulmonary hemorrhage in patients undergoing percutaneous CT-guided transthoracic lung biopsy: single-institution experience of 1175 cases. Radiology. 2016;279(1):287–96.
5. Wolf FJ, Dupuy DE, Machan JT, et al. Adrenal neoplasms: effectiveness and safety of CT-guided ablation of 23 tumors in 22 patients. Eur J Radiol. 2012;81(8):1717–23.
6. Arellano RS, Gervais DA, Mueller PR. CT-guided drainage of abdominal abscesses: hydrodissection to create access routes for percutaneous drainage. Am J Roentgenol. 2011;196(1):189–91.
7. Suzuki K, Shimohira M, Hashizume T, et al. Usefulness of CT-guided hookwire marking before video-assisted thoracoscopic surgery for small pulmonary lesions. J Med Imaging Radiat Oncol. 2014;58(6):657–62.
8. Li Q, Liu P, Qi L, et al. A system design of image-guided automated surgery robot. IEEE Int Conf Real-time Comput Robot (RCAR). 2017;2017:378–82.
9. Putzer D, Arco D, Schamberger B, et al. Comparison of two electromagnetic navigation systems for CT-guided punctures: a phantom study. Rofo. 2016;188(5):470–8.
10. Beyer LP, Wiggermann P. Planning and guidance: new tools to enhance the human skills in interventional oncology. Diagn Interv Imaging. 2017;98(9):583–8.
11. de Baere T, Roux C, Noel G, et al. Robotic assistance for percutaneous needle insertion in the kidney: pre interventional surgery proof on a swine animal model. Eur Radiol Exp. 2022;6(1):1–7.
12. Fong AJ, Stewart CL, Lafaro K, et al. Robotic assistance for quick and accurate image-guided needle placement. Updat Surg. 2021;73(3):1197–201.
13. Mbalisike EC, Vogl TJ, Zangos S, et al. Image-guided microwave thermoablation of hepatic tumours using novel robotic guidance: an early experience. Eur Radiol. 2015;25(2):454–62.
14. Abdullah BJ, Yeong CH, Goh KL, et al. Robotic-assisted thermal ablation of liver tumours. Eur Radiol. 2015;25(1):246–57.
15. Smakic A, Rathmann N, Kostrzewa M, et al. Performance of a robotic assistance device in computed tomography-guided percutaneous diagnostic and therapeutic procedures. Cardiovasc Interv Radiol. 2018;41(4):639–44.
16. Groetz S, Wilhelm K, Willinek W, et al. A new robotic assistance system for percutaneous CT-guided punctures: initial experience. Minim Invasive Ther Allied Technol. 2016;25(2):79–85.
17. Hiraki T, Kamegawa T, Matsuno T, et al. Zerobot®: a remote-controlled robot for needle insertion in CT-guided interventional radiology developed at Okayama university. Acta Med Okayama. 2018;72(6):539–46.
18. Hiraki T, Kamegawa T, Matsuno T, et al. Robotically driven CT-guided needle insertion: preliminary results in phantom and animal experiments. Radiology. 2017;285(2):454–61.
19. Guiu B, De Baère T, Noel G, et al. Feasibility, safety and accuracy of a CT-guided robotic assistance for percutaneous needle placement in a swine liver model. Sci Rep. 2021;11(1):1–11.
20. Lanouzière M, Varbédian O, Chevallier O, et al. Computed tomography-navigation^{TM} electromagnetic system compared to conventional computed tomography guidance for percutaneous lung biopsy: a single-center experience. Diagnostics. 2021;11(9):1532.
21. Tacher V, Blain M, Hérin E, et al. CBCT-based image guidance for percutaneous access: electromagnetic navigation versus 3D image fusion with fluoroscopy versus combination of both technologies—a phantom study. Cardiovasc Interv Radiol. 2020;43(3):495–504.
22. Zhang Z, Shao G, Zheng J, et al. Electromagnetic navigation to assist with computed tomography-guided thermal ablation of liver tumors. Minim Invasive Ther Allied Technol. 2020;29(5):275–82.
23. Huo YR, Chan MV, Habib AR, et al. Pneumothorax rates in CT-guided lung biopsies: a comprehensive systematic review and meta-analysis of risk factors. Br J Radiol. 2020;93(1108):20190866.
24. Wiener RS, Wiener DC, Gould MK. Risks of transthoracic needle biopsy: How high? Clin Pulm Med. 2013;20(1):29.